

# Chaotic spin-dependent electron dynamics in a field-driven double dot potential

L. Chotorlishvili,<sup>1,2</sup> Z. Toklikishvili,<sup>3</sup> A. Komnik,<sup>2</sup> and J. Berakdar<sup>1</sup>

<sup>1</sup> *Institut für Physik, Martin-Luther Universität Halle-Wittenberg,  
Heinrich-Damerow-Str.4, 06120 Halle, Germany*

<sup>2</sup> *Institut für Theoretische Physik, Universität Heidelberg,  
Philosophenweg 19, D-69120 Heidelberg, Germany*

<sup>3</sup> *Physics Department of the Tbilisi State University,  
Chavchavadze av.3, 0128, Tbilisi, Georgia*

## Abstract

We study the nonlinear classical dynamics of an electron confined in a double dot potential and subjected to a spin-orbit coupling and a constant external magnetic field. It is shown that due to the spin orbit coupling, the energy can be transferred from the spin to the orbital motion. This naturally heats up the orbital motion which, due to the presence of the separatrix line in the phase space of the system, results in a motion of the electron between the dots. It is shown that depending on the strength of the spin orbit coupling and the energy of the system, the electronic orbital motion undergoes a transition from the regular to the chaotic regime.

## I. INTRODUCTION

The development of nanoscience, nanotechnology, and of the design of appropriate systems for quantum information devices [1–6] have triggered a large body of studies on the efficient and the controlled states preparation of systems at the nanoscale. In particular, magnetic nanostructures were demonstrated to be highly promising both from an applied [7–10] and fundamental nonlinear physics [11, 12] point of views. In this respect semiconductor quantum dots with a spin-orbit coupling offer are a good case study [13–15]. A key element in these systems is the coupling of the electron momentum to its spin via the spin orbit (SO) coupling. A momentum dependent coupling offers a new way of manipulating the electron spin by influencing the electron momentum via an external periodic electric field. This is the idea of the electric-dipole spin resonance proposed by Rashba and Efros for the electrons confined in lateral systems on the spatial scale between 10 and 100 nm [15]. However, a strong external electric field can considerably influence the orbital dynamics and drive the system far beyond of the linear regime [16]. Usually nonlinearity implies a complicated behavior and difficulties may arise describing the dynamics [16]. However, the nonlinearity may lead, on the other hand, to a variety of interesting and subtle phenomena [17–20] that have been discussed for a range of physical systems [1–6]. Two aspects are of interest here: First, what defines the regimes where the systems exhibit strongly nonlinear behavior and possibly chaos, and secondly, whether these nonlinearities and the chaotic behavior can be utilized for application as lead to qualitatively new features in the dynamics.

Here we address the first of these questions for the nonlinear electronic dynamics where the driving force is a constant external magnetic field. Thus, we consider an effect opposite to the electron-dipole spin resonance protocol offered by Rashba and Efros [15]. In particular, we will consider the dynamics of the electron with SO coupling term, confined in the quantum dot and subjected to the action external magnetic field. Via the external magnetic field, one can directly control the spin dynamics and therefore eventually influence the orbital motion. We will show that under different conditions, depending on the fields parameters and the strength of the SO coupling, different types of the dynamics can be realized. These various types of the dynamics will be linked to the structure of the phase space of the system. We will demonstrate that using driving external fields one can switch the chaotic behavior in the orbital motion on and off.

## II. MODEL

We consider a model system: An electron with mass  $m_e$  is being confined to a double quantum well described by a potential of the form  $U(x) = U_0 [-2(x/d)^2 + (x/d)^4]$ . Here  $U_0$  is the energy barrier, and  $2d$  is the distance between the minima. We will consider the low temperature limit in which case the orbital dynamics is not sensitive to the thermally assisted tunneling. For the particular values of the parameters  $d \sim 100$  nm and  $U_0 \sim 20$  meV this imposes the following restriction on the temperature  $T < 100$  K. For the typical for GaAs electron effective mass  $m_e = 0.067m_0$  the semiclassical tunneling probability is small, namely  $\exp\left[-\frac{8\sqrt{2d m_e U_0}}{3}\right] \approx 10^{-4}$ . Therefore, a classical consideration is justified. To quantify the SO interaction we use the Dresselhaus type coupling term  $H_{so} = \alpha p \sigma_x$ , where  $p$  is the electron momentum, and we assume  $\hbar \equiv 1$ . Consequently the Hamiltonian of the system, with the applied external magnetic  $B(t)$  being parallel to the  $z$ -axis, reads

$$H = \frac{p^2}{2m_e} + U(x) + \alpha p \sigma_x + \mu_B g B(t) \frac{\sigma_z}{2}, \quad (1)$$

where  $\mu_B$  is the Bohr magneton, and  $g$  is the electron Landé factor. Introducing the characteristic maximum momentum  $p^{\max} = \sqrt{2m_e U_0}$  we can estimate the maximal precession rate due to the SO coupling term  $\Omega_{so}^{\max} = 2\alpha\sqrt{2m_e U_0}$ . While a constant magnetic field of the amplitude  $B(t) = B$ , induces a spin precession around  $z$ -axis with the frequency  $\Omega_B = \mu_B g B$ . Therefore, if the amplitude of the magnetic field is strong enough  $B > 2\alpha\sqrt{2m_e U_0}/\mu_B g$ ,  $\Omega_B > \Omega_{so}^{\max}$  the spin dynamics is described by the relation  $\sigma_x(t) = \sigma_x^{(0)} \cos(\Omega_B t)$  and the Hamiltonian (1) takes on the form

$$H = \frac{p^2}{2m_e} + U(x) + \alpha p \cos(\Omega_B t), \quad (2)$$

$$\sigma_x(t) \equiv \cos(\Omega_B t), \quad \sigma_x^{(0)} = 1.$$

In what follows, we will treat time dependent term in (2) as a perturbation and for the sake of convenience we use dimensionless units by introducing the scaling:  $E \rightarrow E/4U_0$ ,  $x \rightarrow x/d$ ,  $t \rightarrow \Omega_B t$ ,  $p \rightarrow p/\sqrt{2m_e U_0}$ ,  $\alpha \rightarrow \alpha\sqrt{m_e/4U_0}$ .

### III. SOLUTION OF THE AUTONOMOUS SYSTEM: STRUCTURE OF THE PHASE SPACE

Before treating the general time dependent problem, we consider the autonomous system and find the corresponding solutions. This allows to identify the topological structure of the phase trajectories. For the autonomous case  $\alpha = 0$  the equation of motion corresponding to the Hamiltonian (2) reads

$$\dot{p}_x = -\frac{\partial H}{\partial x} = x - x^3. \quad (3)$$

Performing the integration in (3) and inverting the result, for energies  $E$  near the potential minimum we obtain an oscillatory behavior in the form

$$x(t) = \pm \sqrt{x_1^2 + (x_0^2 - x_1^2) \text{cn}^2(x_0 t / \sqrt{2}; k)}, \quad -\frac{1}{4} < E < 0. \quad (4)$$

Here  $x_{0,1}$ ,  $x_0 = \sqrt{1 + \sqrt{1 + 4E}}$ ,  $x_1 = \sqrt{1 - \sqrt{1 + 4E}}$ ,  $x_1^2 = 2 - x_0^2$  are the turning points defined by the relation  $V(x) = E$ ,  $\text{cn}(\dots)$  is the elliptic Jacobi cosine [21], and the parameter  $k$  has the form  $k^2 = (x_0^2 - x_1^2) / x_0^2$ . Close to the separatrix we have  $E = 0$  and consequently  $k = 1$ . If the energy of the system is negative, then the electron is located in the left or in the right well and performs oscillation confined by the potential barrier. The oscillations in the different wells are described by the solutions with different signs in (4). The time of the oscillation is given by  $T_0 = 2\sqrt{2}K(k)/x_0$ , where  $K(k)$  is the complete elliptic integral of the first kind [21]. If the energy of the system is positive, the solution of the equation (3) reads

$$x(t) = x_0 \text{cn}\left(\sqrt{x_0^2 - 1}t, 1/k\right), \quad E > 0. \quad (5)$$

From the solutions (4), (5) we conclude that, depending on the values of the parameter  $K$  the dynamics has qualitatively different nature. They are separated by the value  $K = 1$  of the bifurcation parameter hinting on the presence of topologically distinct solutions (see Fig.1). In the case of a positive energy, the electron can overcome the potential barrier and undergoes inter-minima transitions, e.g. from the left to the right minima. The separatrix line that divides different types of solutions corresponds to the zero energy case  $E = 0$  and the separatrix solutions have the following form:

$$x = \frac{\sqrt{2}}{\cosh(t)}, \quad p = -\frac{\tanh(t)}{\cosh(t)}. \quad (6)$$

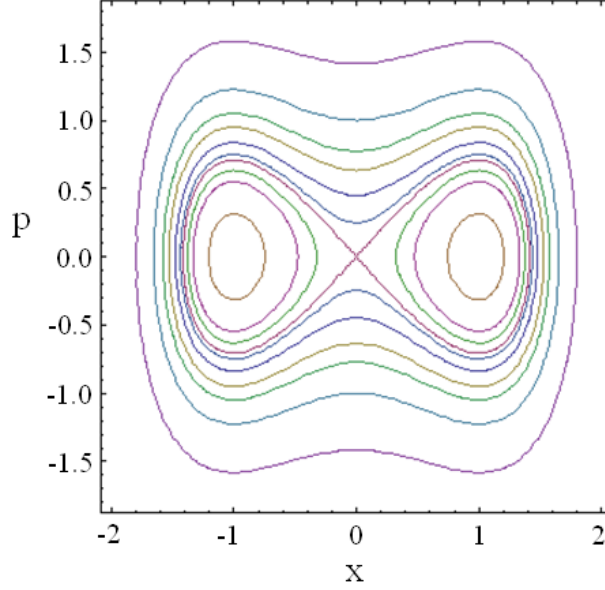


FIG. 1. Phase portrait of the system (3). The phase trajectories with negative or positive values of the coordinate  $x < 0$ ,  $x > 0$  describe the dynamics of the electron located on the left or the right well, respectively. These phase trajectories are separated by a separatrix line from the trajectories corresponding to the positive energy case. The separatrix crossing the nodal point ( $p = 0, x = 0$ ) belongs to the area of a maximal chaos and arises if an external perturbation is applied.

The dynamics near the separatrix is very sensitive to small perturbations. This fact can be exploited to help the electron overcome the potential barrier and to perform a transition between two equilibrium minima. The role of such a perturbation in our case is played by the SO term in (2). The physical mechanism behind the switching of the electron position between the minima points is the formation of a homoclinic structure. Homoclinic structure is formed due to the applied perturbation in the vicinity of the separatrix crossing the nodal point. The formation of the homoclinic structure can be verified via the Melnikov function method [22]. The equations of motion for a perturbed system can be represented in the following general form

$$\begin{aligned}\dot{x} &= \frac{\partial H_0}{\partial p} + \alpha f(x, p, t), \\ \dot{p}_x &= -\frac{\partial H_0}{\partial x} + \alpha g(x, p, t).\end{aligned}\tag{7}$$

Here the terms  $H_x = \partial H_0 / \partial x$ ,  $H_p = \partial H_0 / \partial p$  describe the unperturbed motion, while the contribution from the spin-orbit coupling are contained in the terms  $\alpha f(x, p, t)$  and

$\alpha g(x, p, t)$ . Taking into account (2) we immediately see  $f = \cos(t)$  and  $g = 0$ . Using (7) we can write Melnikov's integral in the following form

$$\Delta(\theta) = \int_{-\infty}^{+\infty} [H_x(x, p)f(x, p, t) + H_p(x, p)g(x, p, t)] dt. \quad (8)$$

Melnikov integral is a measure of the distance between perturbed stable and perturbed unstable separatrix trajectories. Therefore, a change of the sign of the Melnikov integral is equivalent to the crossing of the stable and unstable separatrix trajectories. Consequently, the formation of the homoclinic structure can be identified as the change of the sign of the Melnikov integral. On the other hand, a crossing of the separatrix is equivalent to a transition between the minima of the potential well. Introducing a shift of the initial moment of time  $t \rightarrow t + \theta$  we can obtain the one dimensional parameterization for an ensemble of the separatrix trajectories and for the distances between the trajectories as well. Using the shifted separatrix solutions

$$x = \frac{\sqrt{2}}{\cosh(t + \theta)}, \quad p = -\frac{\tanh(t + \theta)}{\cosh(t + \theta)}, \quad (9)$$

from (8) we obtain:

$$\Delta(\theta) = \frac{\alpha\pi\sqrt{2}}{\cosh(\pi/2)} \cos(\theta). \quad (10)$$

From (10) we see that the dimensionless switching time is equal to the  $\theta \approx \pi$ . Therefore, taking into account the connection between the real and the dimensionless time  $\theta \rightarrow \theta \cdot \Omega_B$  we conclude that the real switching time is proportional to the inverse precession rate  $\theta \approx \pi/\Omega_B \approx T$ . However, note that the switching happens only close to the separatrix and the system needs an additional time to reach the separatrix state. The time that the system needs to reach the separatrix state should be larger than  $\theta \approx \pi/\Omega_B$ . This can be checked by numerical calculations as well (see Fig. 2 and Fig. 3)

#### IV. WIDTH OF STOCHASTIC LAYER AND CRITERIA OF CHAOS

As was mentioned above, the SO interaction should lead to the formation of a stochastic layer in the vicinity of the separatrix line [22]. The finite width of the stochastic layer can be evaluated using the theoretical approach developed in the papers [23, 24]. Since the separatrix divides the phase space in two parts  $\sigma = (\text{in}, \text{out})$ , the perturbation  $V(t) =$

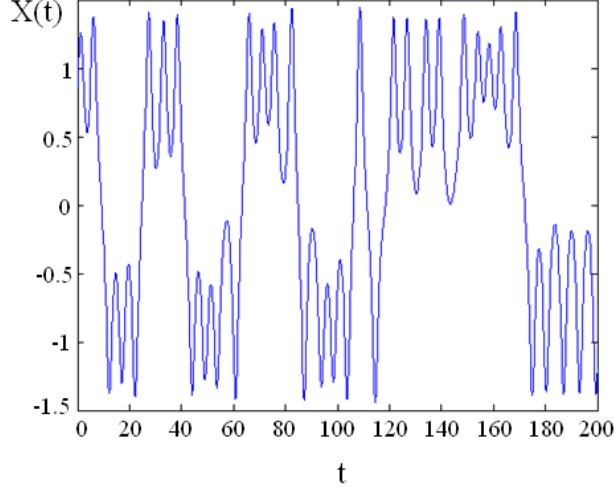


FIG. 2. Numerical solutions of the system described by eq. (2). The generated chaotic trajectory lies close to the separatrix  $E = 0.01$ ,  $\Omega_B = 1$ ,  $\alpha \rightarrow \alpha/4U_0 = 0.2$

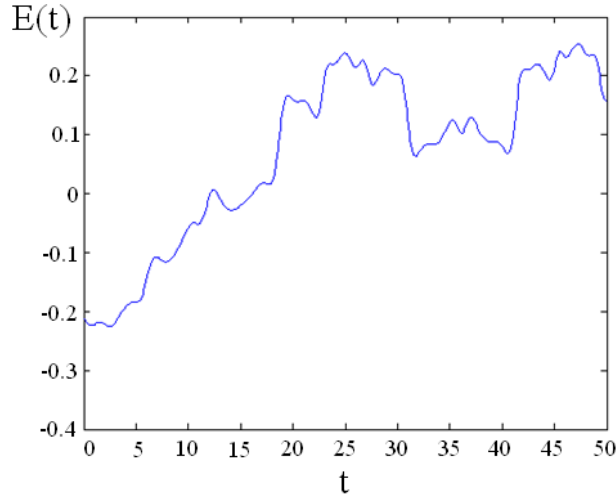


FIG. 3. In order to reach the separatrix value of the energy  $E \approx 0$ , the system needs a time which is clearly larger than the inverse precession frequency  $t > 1/\Omega_B$ ,  $\Omega_B = 1$ ,  $\alpha = 0.2$

$\alpha p \cos(\Omega_B t)$  leads to the formation of a stochastic layer on both sides of the separatrix, see Fig. 4. In what follows we refer to the inner and outward parts of the stochastic layer by the index (*in*, *out*), respectively. The inverse precession frequency  $1/\Omega_B$  defines the time scale of the dimensionless time and therefore we set  $\Omega_B = 1$ .

The change of the energy of the system  $H_0$  and the angular variable  $\varphi$  during one oscillation period  $T_\sigma$  forms the discrete map  $(E_i; \varphi_i) \rightarrow (E_{i+1}; \varphi_{i+1})$ ,  $t_i \rightarrow t_{i+1} = t_i + T_\sigma$ ,  $\sigma = (\text{in}, \text{out})$ .

$$E_{i+1} = E_i + \Delta H^\sigma(\varphi_i); \quad \varphi_{i+1} = \varphi_i + \Delta \varphi^\sigma(E_{i+1}), \quad (11)$$

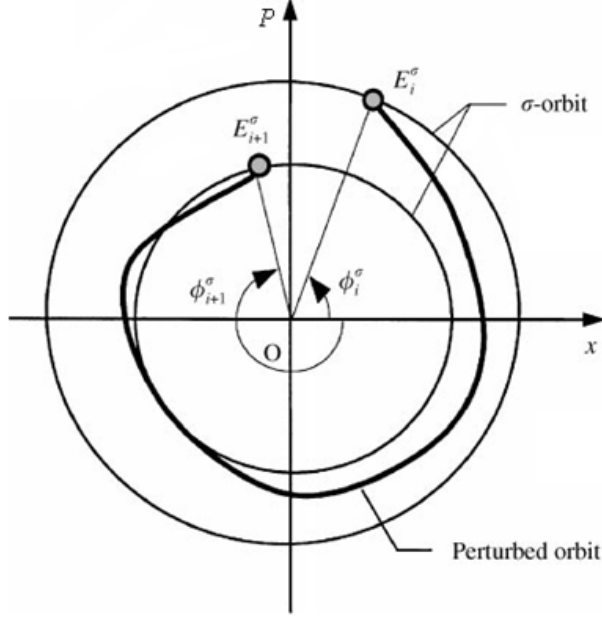


FIG. 4. Perturbed trajectories in the vicinity of the separatrix [24].

where  $E_i = H(x(t_i), p(t_i))$ ,  $\varphi_i = \varphi(x(t_i), p(t_i))$  and  $\Delta H^\sigma(\varphi_i)$ ,  $\Delta\varphi^\sigma(E_{i+1})$  are the increment of the energy and the phase during one period that may occur due to the applied perturbation. The change of the phase and the energy of the system  $\Delta\varphi^\sigma(E_{i+1})$ ,  $\Delta H^\sigma(\varphi_i)$  can be evaluated via the following equations

$$\Delta\varphi^\sigma \approx \Omega_B T_\sigma(E_{i+1}), \quad \Delta H^\sigma(\varphi_i) \approx \int_{t_i}^{t_i + T_\sigma(E_i)} \{H_0, V\} dt. \quad (12)$$

Here  $\{H_0, V\}$  is the Poisson bracket. Due to the nonlinearity, the frequency of the orbital motion depends on the energy of the system with  $\omega_\sigma = 2\pi/T_\sigma(E)$ . Therefore, the resonance condition with the external perturbation in case of nonlinear system has the form  $m_\sigma \omega_\sigma = n_\sigma \Omega_B$ . Here  $n_\sigma$ ,  $m_\sigma$  are integer numbers. The fixed points for the particular resonance ( $m_\sigma : n_\sigma$ ) are defined via the following equations:

$$E_{i+1} = E_i = E_\sigma^{m_\sigma : n_\sigma}, \quad (13)$$

$$\Delta\varphi^\sigma(E_\sigma^{(m_\sigma : n_\sigma)}) \approx \frac{2\pi m_\sigma}{n_\sigma}, \quad \Delta H^\sigma(\varphi_\sigma^{(m_\sigma : n_\sigma)}) = 0. \quad (14)$$

From (13) one can define resonant values of the phase  $\varphi_\sigma^{(m_\sigma : n_\sigma)}$  and energy  $E_\sigma^{(m_\sigma : n_\sigma)}$ . Energy of the system itself can be presented as a sum of the resonant part  $E_\sigma^{(m_\sigma : n_\sigma)}$  and deviation  $\Delta E_i$

$$E_i = E_\sigma^{(m_\sigma : n_\sigma)} + \Delta E_i. \quad (15)$$



Using (15) we can rewrite map (11) in the form

$$\begin{aligned}\Delta E_{i+1} &= \Delta E_i + \Delta H^\sigma(\varphi_i), \\ \varphi_{i+1} &= \varphi_i + \Delta\varphi^\sigma(E_{i+1}) = \varphi_i + \left. \frac{\partial \Delta\varphi(E_{i+1})}{\partial E_{i+1}} \right|_{E_{i+1}=E_\sigma^{(m_\sigma:n_\sigma)}} \Delta E_{i+1}.\end{aligned}\tag{16}$$

With the notations

$$\begin{aligned}G_\sigma^{(m_\sigma:n_\sigma)} &= \left. \frac{\partial \Delta\varphi(E_{i+1})}{\partial E_{i+1}} \right|_{E_{i+1}=E_\sigma^{(m_\sigma:n_\sigma)}}, \\ I_i &= G_\sigma^{(m_\sigma:n_\sigma)} \cdot \Delta E_i,\end{aligned}\tag{17}$$

Eq. (16) can be rewritten in the following form

$$\begin{aligned}I_{i+1} &= I_i + G_\sigma^{(m_\sigma:n_\sigma)} \cdot \Delta H^\sigma(\varphi_i), \\ \varphi_{i+1} &= \varphi_i + I_{i+1}.\end{aligned}\tag{18}$$

Using (3), (9) and (12) one can derive the explicit expression for the change of the energy of the system  $H_0$ , during one oscillation period  $T_\sigma$ :

$$\begin{aligned}\Delta H^\sigma(\varphi_i) &\approx \int_{t_i}^{t_i+T_\sigma(E_i)} \{H_0, V\} dt = \\ &= \alpha \left( \int_{-\infty}^{+\infty} dt \frac{2\sqrt{2} \cos \Omega_B t}{\cosh^3[\Omega_B(t-t_i)]} - \sqrt{2} \int_{-\infty}^{+\infty} dt \frac{2\sqrt{2} \cos \Omega_B t}{\cosh[\Omega_B(t-t_i)]} \right) = \alpha \sqrt{2} \frac{\pi}{\cosh(\pi/2)} \cos \varphi_i, \\ \sigma &= (\text{in}, \text{out}), \quad \varphi_i = t_i.\end{aligned}\tag{19}$$

In (19), due to the time localization of the profile of the solution (9), we extended the limits of integration to infinity. For the evaluation of the phase increment  $\Delta\varphi^\sigma(E_{i+1})$  that occurs during one period, again we note that the separatrix divides the phase space on two parts  $\sigma = (\text{in}, \text{out})$ . For inner area  $\sigma = \text{in}$  in the period of the oscillation, for the solution (4) reads  $T_0 = 2\sqrt{2}K(k)/x_0$ . Therefore, for the phase increment during one period of the oscillation we have  $\Delta\varphi(E_\alpha) = T_0 = 2\sqrt{2}K(k)/x_0$ . Taking into account the logarithmic divergence of the elliptic integral  $K(k \approx \ln(16/(1-k^2))/2)$  and the relations  $x_0 = \sqrt{2}$ ,  $1-k^2 = -E_{in} = |E_{in}|$ , the phase increment that occurs during one oscillation period, for the trajectory in the vicinity of the separatrix reads  $\Delta\varphi(E_{in}) = T_{in} = \ln(16/|E_{in}|)$ . Taking into account this fact, for the explicit form of the map (11) we deduce

$$\varphi_{i+1} = \varphi_i + \ln \left( \frac{16}{|E_{i+1}|} \right),\tag{20}$$

$$E_{i+1} = E_i + \alpha \sqrt{2} \frac{\pi}{\cosh(\pi/2)} \cos \varphi_i.\tag{21}$$

In particular, for the fixed points of the first resonance ( $m_\sigma : 1_\sigma$ ) from (20) we deduce:

$$E_{i+1} = E_i = E_{in}^{m:1}, \quad \varphi_{i+1} = \varphi_i + 2\pi m = \varphi_{in}^{m:1} + 2\pi m. \quad (22)$$

From (22) we obtain

$$\alpha\sqrt{2}\frac{\pi}{\cosh(\pi/2)}\cos\varphi_{in}^m = 0, \quad \ln\left(\frac{16}{|E_{in}^m|}\right) = 2m\pi. \quad (23)$$

Taking into account (23) we find

$$\varphi_\alpha^m = \frac{\pi}{2} + k\pi, k \in N, \quad |E_\alpha^m| = 16e^{-2m\pi}. \quad (24)$$

Using (24) we can rewrite the map (20) in the vicinity of the fixed points in the following form

$$\begin{aligned} I_{i+1} &= I_i - K_m \sin \theta_i, \\ \theta_{i+1} &= \theta_i + I_{i+1}. \end{aligned} \quad (25)$$

Here

$$K_m = \frac{\alpha\sqrt{2}}{|E_{in}^m|} \frac{\pi}{\cosh(\pi/2)}, \quad (26)$$

is the coefficient of the stochasticity and for convenience we used the new variable with the shifted phase  $\theta_i = \varphi_i + \pi/2$ . The continuous limit of the map (25) reads

$$\begin{aligned} \frac{dI}{di} &= -K_m \sin \theta, \\ \frac{d\theta}{di} &= I, \end{aligned} \quad (27)$$

where the index  $i$  plays the role of time. The differential equations (27) can be derived straightforwardly from the effective Hamiltonian

$$H_{\text{eff}} = \frac{1}{2}I^2 + K_m \sin \theta. \quad (28)$$

On the other hand, the effective Hamiltonian responsible for the map (26) reads

$$H'_{\text{eff}} = \frac{1}{2}I^2 - K_m \cos \theta \sum_{\nu=-\infty}^{\infty} \delta(t - \nu). \quad (29)$$

The separatrix energy for the Hamiltonian (28) is equal to the coefficient of the stochasticity for the map (25)  $E_s = K_m$  [22]. In addition, we note that the equivalence of our system (26) to the effective Hamiltonian (30) is very helpful. Since for the evolution of the width

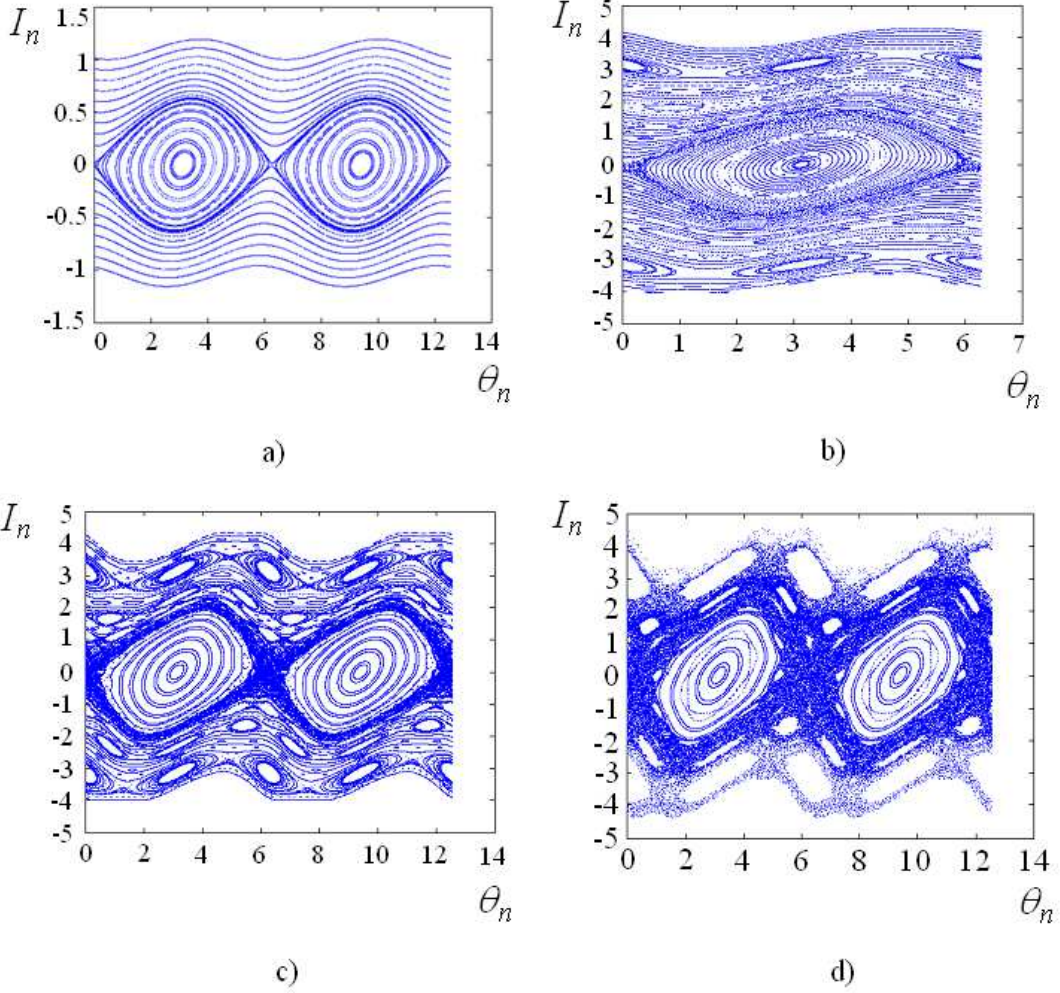


FIG. 5. The phase portrait of the system given by eq. (25). About 200 trajectories are generated for the different values of the stochastic parameter  $K$ : a)  $K = 0.1$ , b)  $K = 0.7$ , c)  $K = 1$ , d)  $K = 1.2$ .

of the stochastic layer for our system we simply can adopt the well-known results for the system [25] (30). In our derivations we have considered the trajectory that lies in the vicinity of the separatrix of the initial system (3) (see Fig.4). Therefore, in our derivation  $E_{in}^m$  is supposed to be small however different from zero. The reason is that exactly on the separatrix  $E_{in}^m = 0$  of the initial system (3) a motion is impossible since the period of the oscillation diverges logarithmically  $T_{in} = \ln(16/|E_{in}^m|) \rightarrow \infty$ ,  $E_{in}^m \rightarrow 0$ . Consequently, the coefficient of the stochasticity (26) is large but finite. Using (24) we can rewrite the coefficient of the stochasticity in the following form

$$K_m = \frac{\alpha\sqrt{2}}{16} e^{2m\pi} \frac{\pi}{\cosh(\pi/2)}. \quad (30)$$

From Eq. (30) we can easily infer the connection between the amplitude of the SO coupling  $\alpha$  and the emergence of chaos. Chaos in the system appears if  $K_m > 1$ .

Taking into account (26) and (30) we obtain

$$\alpha > \sqrt{\frac{4U_0}{m_e} \frac{|E_{in}^m|}{\pi\sqrt{2}}} \cosh(\pi/2). \quad (31)$$

The width of the stochastic layer reads [25]

$$\delta E_m = 2U_0(4\pi)^4 \sqrt{K_m} \exp\left(-\frac{\pi^2}{\sqrt{K_m}}\right). \quad (32)$$

In (31) and (32) we have used the definitions  $E \rightarrow E/4U_0$ ,  $\alpha \rightarrow \alpha\sqrt{m_e/4U_0}$  and from the dimensionless SO constant and the dimensionless energy we switched back to the real SO constant and the energy. The value of the width of the stochastic layer is a very important quantity. Since  $\delta E_m$  defines the width of the energy interval where chaos appears  $E > -\delta E_m < E$ . Note that the width of the stochastic layer  $\delta E_m$  depends on the two real physical parameters only: The barrier height  $U_0$  and the SO coupling constant  $\alpha$ . Therefore, the energy when chaos appears in the system can be estimated easily and verified by the experiment. The width of the stochastic layer is proportional to the SO constant. Consequently, the energy window of the chaotic dynamics  $-\delta E_m < E < \delta E_m$  is proportional to the SO constant as well. From (31) we see that the chaos criteria  $K_m > 1$ , connect to several real physical parameters such as the SO coupling constant  $\alpha$ , the height of the potential barrier  $U_0$ , energy of the system, and the effective mass of the electron  $m_e$ . Therefore, the effect of chaos should be easily observable in the experiment by tuning these parameters. Close to the separatrix when the energy of the system tends to zero  $E_{in}^m \rightarrow 0$  the chaos criteria  $K_m > 1$  holds even for the very weak SO interaction which confirms the sensitivity of the system near the separatrix. The simple relations (26)-(32) naturally define a particular class of the materials where the transition from the regular to the irregular orbital dynamics of the electron can be observed easily on the experiment. A phase portrait for the orbital motion of the electron, for the different values of the coefficient of the stochasticity is shown in Fig.5. As we see from Fig. 5 with the increase of the coefficient  $K = K_m$ , the system undergoes a transition from the regular motion Fig.5a) to the irregular one displayed in Fig.5b).

## V. CONCLUSIONS.

In the present project we considered a simple model relevant for spintronics. The electron spin is coupled to the orbital motion via a SO coupling term and is confined in a double quantum dot. For the control of the spin dynamics, we considered a driving protocol based on an external magnetic field applied along  $z$  axis. We have shown that if the amplitude of the applied field is strong enough  $B > 2\alpha\sqrt{2mU_0}/\mu_B g$ , the spin dynamics is periodical in time. In particular, the spin rotates around  $z$  axis with a frequency  $\Omega_B = \mu_B g B$  and for the  $x$  projection of the spin we have  $\sigma_x(t) = \sigma_x^{(0)} \cos(\Omega_B t)$ . Due to this the orbital dynamics can be reduced to an effective, time dependent, one dimensional Hamiltonian model (2). Different types of the dynamics can be realized. If the energy of the system is negative  $-1/4 < E < 0$ , the electron is localized in the right or in the left well and performs oscillations bound by the potential barriers. However, via the spin orbit coupling channel, energy can be transferred from the spin system to the orbital motion. This naturally heats up the orbital motion of the electron and due to the presence of a separatrix line in the phase space of the system (3), the electron may change from one potential well to the other. We call this effect a spin orbit coupling induced "tunneling" (even though this process is not a tunneling in the quantum mechanical sense) to stress the fact that the electron can perform inter-well transitions. We derived simple analytical equations (26)-(32) for the appearance of chaos and showed how this regime can be reached via tuning real physical parameters such as SO coupling constant  $\alpha$ , the height of the potential barrier  $U_0$ , the energy of the system, and the effective mass of the electron  $m_e$ . Therefore, the effect of chaos should be easily observable on the experiment. We also proved that close to the separatrix when the energy of the system tends to zero  $E_{in}^m \rightarrow 0$  the chaos criteria  $K_m > 1$  holds even for a very weak SO interaction, confirming by this the extreme sensitivity of the system near to the separatrix. In addition we derived expression for the width of the stochastic layer (32). We proved that the width of the separatrix is proportional to the SO constant and inversely proportional to the energy of the system.

**Acknowledgments** We thank E.Ya. Sherman for useful discussions. The financial support by the Deutsche Forschungsgemeinschaft (DFG) through SFB 762, contract BE 2161/5-1,

Grant No. KO-2235/3, and STCU Grant No. 5053 is gratefully acknowledged.

---

- [1] J. Raimond, M. Brune, and S. Haroche, *Rev. Mod. Phys.* **73**, 565 (2001).
- [2] S.N. Shevchenko, S. Ashhab, and F. Nori, *Phys. Rep.* **492**, 1 (2010).
- [3] F. Zahringer, G. Kirchmair, R. Gerritsma, E. Solano, R. Blatt, and C.F. Roos, *Phys. Rev. Lett.* **104**, 100503 (2010).
- [4] W. Wernsdorfer, N. Aliaga-Alcalde, D. N. Hendrickson, and G. Christou, *Nature* **416**, 406 (2002).
- [5] G. Heinrich and F. Marquardt, *EPL* **93**, 18003 (2011).
- [6] R. B. Karabalin, M. C. Cross, and M. L. Roukes, *Phys. Rev. B* **79**, 165309 (2009).
- [7] C. F. Hirjibehedin, C. P. Lutz, and A. J. Heinrich, *Science* **312**, 1021 (2006).
- [8] S. Rusponi, T. Cren, N. Weiss, M. Epple, P. Bulushek, L. Claude, and H. Brune, *Nat. Mater.* **2**, 546 (2003).
- [9] T. Mirkovic, M. L. Foo, A. C. Arsenault, S. Fournier-Bidoz, N. S. Zacharia, and G. A. Ozin, *Nat. Nanotechnol.* **2**, 565 (2007).
- [10] J.A. Strosio and R. J. Celotta, *Science* **306**, 242 (2004).
- [11] L. Chotorlishvili, Z. Toklikishvili, A. Komnik, and J. Berakdar, *Phys. Rev. B* **83**, 184405 (2011).
- [12] L. Chotorlishvili, P. Schwab, Z. Toklikishvili, and J. Berakdar, *Phys. Rev. B* **82**, 014418 (2010).
- [13] M. Valin-Rodriguez, A. Puente, L. Serra, and E. Lipparini, *Phys. Rev. B* **66**, 235322 (2002).
- [14] L. S. Levitov and E. I. Rashba, *Phys. Rev. B* **67**, 115324 (2003).
- [15] E. I. Rashba and A. L. Efros, *Phys. Rev. Lett.* **91**, 126405 (2003).
- [16] D. V. Khomitsky and E. Ya. Sherman, *Phys. Rev. B* **79**, 245321 (2009).
- [17] L.E. Reichl and W.M. Zheng, *Phys. Rev. A* **29**, 2186 (1984).
- [18] W.A. Lin and L.E. Ballentine, *Phys. Rev. Lett.* **65**, 2927 (1990), W.A. Lin and L.E. Ballentine, *Phys. Rev. A* **45**, 3637 (1992).
- [19] A. Tameshtit and J. E. Sipe, *Phys. Rev. E* **51**, 1582 (1995), A. Tameshtit and J. E. Sipe, *Phys. Rev. A* **47**, 1697 (1993).
- [20] A. T. Ngo, E. H. Kim, and S. E. Ulloa, arXiv:1103.3265.

- [21] M. Abramowitz and I. Stegun, Handbook of Mathematical Functions (Applied Mathematics Series vol. 55, Washington: National Bureau of Standards, 1972).
- [22] G. M. Zaslavsky, The Physics of Chaos in Hamiltonian Systems (London, Imperial College, 2007).
- [23] A. C. J. Luo, R. P. S. Han, Chaos, Solitons, and Fractals **12**, 2493 (2001).
- [24] A. C. J. Luo, K. Gu, and Ray P. S. Han, Nonlinear Dynamics **19**, 37 (1999).
- [25] G. M. Zaslavsky, R. Z. Sagdeev, and D. A. Usikov, Weak Chaos in Semiregular Structures (Moscow, Nauka, 1991)